
Integrating Segmented Cell Imaging and Molecular Networks for Drug-Specific Analysis in CM4AI

Anonymous Author(s)

Affiliation

Address

email

Abstract

1 Linking cellular morphology to molecular interaction networks remains a central
2 challenge in biomedical Artificial Intelligent (AI). We present a cell-centric
3 framework that integrates object-level detection with Vision Transformer (ViT) embeddings
4 from microscopy with protein–protein interaction (PPI) representations
5 to construct biologically interpretable hierarchies and reveal condition-specific
6 network reconfiguration. Using a semi-automated, agent-oriented workflow, segmentation
7 is executed via an interactive Large Language Model (LLM)-driven agent
8 bridged to high-performance computing, while embedding, integration, and hierarchy
9 construction proceed through reproducible human–LLM collaboration with
10 auditable prompts, code generation, and logged execution. Applied to 12853 high-
11 content images spanning Untreated, Vorinostat-, and Paclitaxel-treated conditions,
12 the approach preserves global biological structure while sharpening signal fidelity
13 relative to whole-image baselines, enabling single-cell resolution of heterogeneity.
14 Across all conditions, the modified pipeline maintained >95% concordance with
15 baseline hierarchies. Gene Ontology analyses recover drug-consistent pathways
16 (e.g., chromatin regulation for Vorinostat; microtubule-associated processes for
17 Paclitaxel) and yield more selective enrichment profiles. The framework establishes
18 a scalable foundation for multimodal integration with additional omics layers and
19 for prospective validation of predicted network rewiring in precision medicine
20 contexts.

21 1 Introduction

22 Linking cellular morphology to molecular interaction networks is a central challenge in systems
23 biology and drug discovery [1, 2]. High-content microscopy provides rich phenotypic readouts [3-5],
24 while protein–protein interaction (PPI) networks encode molecular relationships that govern function
25 [1, 2, 6]. Yet, these modalities are typically analyzed in isolation, limiting our ability to explain how
26 drug-induced morphological changes propagate to network-level rewiring [7, 8]. Overcoming this
27 gap is critical for uncovering mechanisms of action and advancing precision therapeutics [9, 10].

28 This problem presents three significant machine learning challenges with important consequences:
29 (1) **Data heterogeneity**—images and graphs differ fundamentally in structure, making cross-domain
30 representation learning difficult. Without effective integration, morphology–network correspondences
31 are often missed or distorted [11-13]; (2) **Scalability and efficiency**—microscopy datasets contain
32 millions of cells, yet whole-image embeddings are dominated by background regions. This wastes
33 computation, inflates storage, and introduces noise, leading to reduced predictive accuracy [14,
34 15]; and (3) **Interpretability**—without transparent mapping between morphology and molecular
35 pathways, models risk becoming black boxes, limiting biological trust and practical utility [16-17].

36 Existing approaches address these challenges only partially and can be grouped into three categories.
37 **Aggregation-based methods** such as MuSIC fuse imaging with molecular data but collapse features

38 across cell populations, losing single-cell heterogeneity [7]. **Static resources** like OpenCell provide
39 valuable maps of localization and interaction but are not designed as dynamic learning frameworks [8].
40 **Morphology profiling assays** such as Cell Painting and its large-scale derivatives capture phenotypic
41 diversity but do not connect directly to molecular interaction networks [8, 18]. Finally, **multimodal**
42 **contrastive methods** (e.g., MaxFuse, MoCoP) highlight the potential of aligning weakly linked
43 modalities, but they have not been applied to morphology–PPI integration and do not resolve the
44 inefficiency of whole-image embeddings [19, 20].

45 We participated in the NIH-funded Cell Maps for Artificial Intelligence (CM4AI) initiative, which
46 was established to link cellular morphology with PPI networks [21]. While CM4AI demonstrated
47 the promise of multimodal integration, it primarily operated on whole-image embeddings, where
48 large portions of each microscopy image consist of empty background or non-informative regions.
49 Treating entire fields of view as single units forced the model to allocate capacity to irrelevant pixels,
50 diluting the signal from actual cellular structures. Moreover, features were aggregated at the image
51 or population level, which masked single-cell variability that is critical for capturing heterogeneity
52 in drug response. As a result, background noise reduced predictive accuracy, and averaging across
53 populations obscured subtle but biologically important differences between individual cells.

54 Our contributions are as follows:

- 55 • **Object-centric embedding pipeline:** A segmentation and embedding pipeline that re-
56 duces background noise and improves the signal-to-noise ratio, leading to more faithful
57 representations of cellular morphology and improved downstream predictive accuracy of
58 morphology–PPI alignment.
- 59 • **Agent-based orchestration:** We develop a semi-automated agent architecture where (Large
60 Language Model) LLMs generate, refine, and execute code in collaboration with human
61 researchers. This orchestration—detailed in the method section—establishes a reproducible
62 workflow that goes beyond simple chaining of off-the-shelf components and represents a
63 methodological advance for AI-driven scientific pipelines.
- 64 • **Cross-domain alignment:** We present novel preprocessing, mapping, and validation pro-
65 cedures for integrating morphology and network embeddings, including ontology-based
66 evaluation with Gene Ontology (GO) analysis.

67 The rest of this article is organized as follows. Section 2 details the proposed methodology, beginning
68 with the multi-agent architecture and then describing algorithms for each pipeline stage: object
69 detection and segmentation, feature extraction, PPI embedding, multimodal integration, and hierarchy
70 generation. Section 3 presents results on drug-specific datasets, including baseline vs. modified
71 pipelines, network analyses, and Gene Ontology/KEGG enrichment. Section 4 examines biological
72 and computational implications, limitations, and future directions. Finally, Section 5 concludes and
73 highlights broader applications in systems biology and precision medicine.

74 2 Proposed Methods

75 2.1 Multi-Agent Architecture Implementation for CM4AI

76 The CM4AI pipeline proceeds through seven auditable stages for integrating cellular morphology
77 with molecular interaction networks: (1) experimental condition parsing and dataset registration, (2)
78 microscopy image ingestion and pre-processing, (3) object detection and LLM-guided segmentation,
79 (4) feature extraction using Vision Transformers (ViT) at the single-cell level, (5) protein–protein
80 interaction (PPI) embedding generation via graph-based models, (6) multimodal contrastive co-
81 embedding with alignment scoring, and (7) hierarchical map construction with ontology-based
82 validation. Execution was coordinated manually by the researchers with LLM assistance rather than
83 by a centralized orchestrator: stage (3) used an interactive agent via a web interface bridged to the
84 High-Performance Computing (HPC) system, whereas stages (4)–(7) were run from user-invoked
85 scripts generated or refined by ChatGPT (and, where noted, Gemini). Transparent logging, metadata
86 propagation, and reproducibility tracking were implemented through scripts and notebooks (e.g.,
87 recorded prompts/configurations, fixed seeds, saved checkpoints), ensuring each step is auditable
88 across imaging and network data modalities.

89 Table 1 highlights the balance of human and AI involvement across the CM4AI pipeline.

90 a-Manual execution of pre-existing scripts written by human researchers.b-No code involved; task
 91 consisted of visual/manual inspection of generated networks.

92

Table 1: Human vs. AI involvement per pipeline stage.

Stg	Activity	AI code (%)	Human code (%)	Executor Manual (%)	Executor Agent (%)
1	Planning	~80	~20	100	0
2	Manuscript	~80	~20	100	0
3	Detection & Segmentation	~95	~5	30	70
4	ViT features extraction	~95	~5	100	0
5	PPI embedding & Co-embedding ^a	0	100	100	0
6	Hierarchy generation	50	50	100	0
7	Ontology check ^b	0	0	100	0

93

94 2.1.1 PlanningAgent

95 The PlanningAgent was used to outline the overall research workflow and formulate experimental
 96 ideas. Through prompt-driven instructions, ChatGPT proposed stepwise pipelines, suggested al-
 97 ternative methodological options, and generated schematic drafts of module interactions. Beyond
 98 technical planning, ChatGPT was also used to brainstorm research directions, especially to identify
 99 innovative approaches for emerging fields. For example, we prompted ChatGPT with the request:
 100 “*You are an expert in drug discovery and computer vision. Propose an approach that could achieve*
 101 *a breakthrough.*”, which generated candidate directions that were later refined. Some preliminary
 102 studies were planned and carried out during this stage before the framework reached its current
 103 milestone. These outputs were not executed directly but served as planning material that the user
 104 evaluated, modified, and selected for implementation. Thus, the agent functioned as an ideation
 105 and organizational support tool rather than an autonomous decision-maker, with final choices and
 106 experimental designs determined by the human researcher.

107 2.1.2 ManuscriptAgent

108 The ManuscriptAgent supported manuscript preparation by generating draft text, structuring sections
 109 in L^AT_EX, suggesting titles and figure captions, and providing language refinement. While ChatGPT
 110 produced most of the drafting and formatting support, some parts (e.g.: Introduction and Proposed
 111 Method) of the paper were written using Gemini through its agent API, which enabled iterative
 112 refinement of specific sections via repeated prompt–response cycles. The user remained responsible
 113 for verifying content accuracy, correcting hallucinated references, and ensuring logical consistency.
 114 In practice, the ManuscriptAgent accelerated drafting and improved readability, but the final paper
 115 required substantial human oversight and revision, reflecting a collaborative human–LLM writing
 116 process rather than a fully automated system.

117 2.1.3 SegmentationAgent

118 We first prompted ChatGPT to perform cell segmentation on the images, and then requested the
 119 corresponding source code. For instance, we used prompts such as: “*You are an expert in the field of*
 120 *biomedical image analysis. Provide bounding boxes for the cells in this image.*” Next, we executed
 121 segmentation of all images through a ChatGPT-provided agent workspace running in a web interface
 122 bridged to our institute’s HPC server, using stepwise, prompt-driven instructions. At each step, we
 123 supplied the agent with specifications (dataset layout, channel usage, output schema, and test criteria),
 124 and the agent generated environment setup scripts (conda/pip with PyTorch, OpenCV, and other
 125 libraries), and executable code for object localization. After pilot verification on sample images, the
 126 agent launched batched jobs across the full dataset, streamed logs/metrics, and wrote masks, boxes,
 127 and cell crops with provenance and metadata. When failures occurred, such as technical errors (e.g.,

128 missing files, broken dependencies) or operational mistakes (e.g., the agent clicking an incorrect
129 button and failing to correct the action in the web interface), the user had to manually take control of
130 the screen to recover and continue execution. Thus, the system operated as a human–LLM co-pilot
131 rather than a fully autonomous agent.

132 2.1.4 EmbeddingAgent

133 The EmbeddingAgent was responsible for generating feature representations from both cell images
134 and protein interaction data. For cell morphology, a ViT backbone was used to extract features,
135 relying on a combination of existing libraries and code generated by ChatGPT in response to prompt
136 instructions. Unlike the segmentation stage, this module was not executed through an autonomous
137 agent interface; instead, ChatGPT produced scripts that the user manually executed on the HPC server.
138 Some preprocessing was handled manually, and errors in processing occasionally required refinement
139 of the code or reruns. Thus, while ChatGPT assisted in code generation and troubleshooting, the
140 embedding stage remained largely user-driven rather than agent-operated.

141 2.1.5 CoEmbeddingAgent and HierarchyAgent

142 The CoEmbeddingAgent was responsible for aligning image-derived embeddings with protein
143 interaction embeddings, while the HierarchyAgent organized the integrated features into higher-level
144 biological groupings. In both cases, previously generated scripts were reused and adapted with minor
145 modifications based on new prompt instructions, rather than written entirely from scratch. These
146 scripts were executed manually on the HPC, with ChatGPT providing refinements and troubleshooting
147 support, but without reliance on a fully autonomous interface.

148 2.2 Modified Pipeline

149 2.2.1 Input Data

150 We constructed a dataset \mathcal{D} composed of approximately 12853 microscopy images:

$$\mathcal{D} = \{(I_i, c_i)\}_{i=1}^N, \quad N \approx 12853 \quad (1)$$

151 where $I_i \in \mathbb{R}^{H \times W \times C}$ is a high-resolution fluorescence microscopy image and $c_i \in$
152 $\{\text{Untreated, Paclitaxel, Vorinostat}\}$ denotes the experimental condition.

153 2.2.2 Object Detection and Segmentation.

154 Raw images contain multiple nuclei, and global embeddings risk averaging out informative local
155 variations. To address this, we applied an LLM-guided object detection function f_{det} that isolates
156 nuclei at the single-cell level, $\mathcal{S}_i = f_{\text{det}}(I_i) = \{s_{i1}, s_{i2}, \dots, s_{iM_i}\}$, where M_i is the number of
157 detected objects in I_i and each segment s_{ij} corresponds to a nucleus or cell mask. This step preserves
158 subtle morphological features, such as nuclear size and chromatin condensation, that are often lost at
159 the global scale.

160 2.2.3 Feature Extraction.

161 Each segment s_{ij} is embedded using a Vision Transformer (ViT) as $\mathbf{z}_{ij}^{\text{img}} = f_{\text{ViT}}(s_{ij}; \theta_{\text{ViT}}) \in \mathbb{R}^{d_{\text{img}}}$,
162 where θ_{ViT} are the learned parameters. The ViT partitions s_{ij} into patches, encodes them as tokens,
163 and applies multi-head self-attention to capture both local and global dependencies.

164 2.3 PPI Embedding

165 To incorporate molecular context, we constructed a protein–protein interaction (PPI) graph $G =$
166 (V, E) , where V denotes proteins and E their interactions. Using a graph embedding function f_{PPI} ,
167 each protein $p \in V$ was mapped to a vector $\mathbf{z}_p^{\text{ppi}} = f_{\text{PPI}}(G; p) \in \mathbb{R}^{d_{\text{ppi}}}$. These embeddings preserve
168 both local and global network structure, such that inner products $\langle \mathbf{z}_u^{\text{ppi}}, \mathbf{z}_v^{\text{ppi}} \rangle$ reflect the likelihood of
169 interaction between proteins u and v .

170 **2.4 Co-Embedding (Multimodal Integration)**

171 To integrate protein image and PPI embeddings into a shared space, we applied the MUSE (*Multi-*
172 *modal Unsupervised Semantic Embedding*) framework. Let $\mathbf{x}_i \in \mathbb{R}^{d_x}$ and $\mathbf{y}_i \in \mathbb{R}^{d_y}$ denote the image
173 and PPI embeddings for protein i in the intersection set \mathcal{I} , which are mapped into a common latent
174 space of dimension d via neural functions f_θ and g_ϕ , yielding $\mathbf{z}_i^{(x)} = f_\theta(\mathbf{x}_i)$ and $\mathbf{z}_i^{(y)} = g_\phi(\mathbf{y}_i)$. For
175 each anchor i , the positive pair $(\mathbf{z}_i^{(x)}, \mathbf{z}_i^{(y)})$ is contrasted against negatives $(\mathbf{z}_i^{(x)}, \mathbf{z}_j^{(y)})$ from the k
176 nearest neighbors ($j \neq i$) using a triplet margin loss $\ell_i = \max(0, \|\mathbf{z}_i^{(x)} - \mathbf{z}_i^{(y)}\|_2 - \|\mathbf{z}_i^{(x)} - \mathbf{z}_j^{(y)}\|_2 + m)$,
177 where m is the margin. The overall objective $\mathcal{L}_{\text{MUSE}} = \sum_{i \in \mathcal{I}} \ell_i + \lambda \Omega(\theta, \phi)$ includes dropout and
178 L2 regularization, and training proceeds in two stages: initialization for n_{init} epochs followed by
179 triplet-based optimization for n_{epochs} epochs. This process aligns image and PPI features of the same
180 protein while enforcing separation from unrelated proteins.

181 **2.5 Hierarchy Generation**

182 The joint embedding matrix was defined as $Z = [\mathbf{z}_{ij}^{\text{joint}}] \in \mathbb{R}^{M \times d}$, and pairwise cosine simi-
183 larities were computed as $\text{sim}(\mathbf{z}_a, \mathbf{z}_b) = \frac{\mathbf{z}_a \cdot \mathbf{z}_b}{\|\mathbf{z}_a\| \|\mathbf{z}_b\|}$. Hierarchical agglomerative clustering was
184 then applied using Ward’s method, where the linkage between clusters A and B is given by
185 $\Delta(A, B) = \frac{|A| \cdot |B|}{|A| + |B|} \|\mu_A - \mu_B\|^2$, with μ_A and μ_B denoting the respective centroids.

186 **3 Results**

187 **3.1 Dataset**

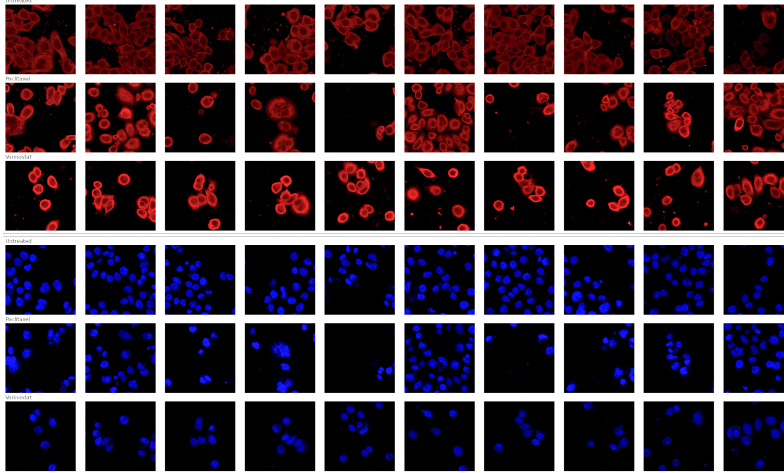


Figure 1: Representative microscopy images from the CM4AI dataset across three experimental conditions: Untreated, Paclitaxel-treated, and Vorinostat-treated.

188 The foundation of our analysis is the publicly available Cell Maps for Artificial Intelligence (CM4AI)
189 dataset, produced under the NIH Bridge2AI Functional Genomics Grand Challenge [21]. As of the
190 June 2025 beta release, CM4AI provides AI-ready RO-Crate archives with rich provenance via the
191 FAIRSCAPE framework.

192 Our study uses the subset of immunofluorescent images of MDA-MB-468 breast cancer cells under
193 three conditions—Untreated, Paclitaxel, and Vorinostat (Fig. 1). Each condition includes microtubule
194 and nuclear channels, which we use for object detection and ViT embedding. CM4AI targets a
195 curated panel of 200 human proteins (100 chromatin modifiers, 100 metabolic enzymes) selected for
196 relevance to cancer, neuropsychiatric, and cardiac disorders, and also provides additional modalities
197 (e.g., proteomics, perturb-seq, spatial proteomics) packaged with interoperable metadata under FAIR
198 principles.

199 **3.2 Hyper-parameter**

200 Our proposed methods were developed using the PyTorch™ framework and implemented on a HPC
 201 running a Red Hat® Enterprise Linux 7 system equipped with two NVIDIA® Tesla™ P100-PCIE-
 202 16GB GPUs and 8 CPU cores (16 GB each) (Table 2). For details of the original pipeline settings,
 203 please refer to a previous publication [21].

Table 2: Experimental settings and hyperparameters.

Module	Parameter	Value
<i>Segmentation</i>		
	GAUSS SIGMA	1.2
	OPEN FOOT	1
	CLOSE FOOT	3
	MIN OBJ FRAC	0.0003
	MIN HOLE FRAC	0.0006
<i>ViT (image features)</i>		
	Backbone	ViT large patch16 224
	Image input size	224
	Feature dim d_{img}	1024
<i>DenseNet (image features)</i>		
	Backbone	DenseNet 121
	Image input size	224
	Feature dim d_{img}	1024
<i>PPI (graph features)</i>		
	Embedding method	Node2Vec
	Feature dim d_{ppi}	1024
<i>Co-Embedding (MUSE)</i>		
	Shared dim d	128
	Margin m	0.1
	Negatives / neighborhood k	10
	Init epochs n_{init}	200
	Total epochs n_{epochs}	500
<i>Compute / Environment</i>		
	GPUs / CPUs / RAM	2/8/128
	Runtime	1 month
	Env hash	conda
<i>Reproducibility</i>		
	Random seeds	42

204 **3.3 Comparison of Baseline and modified CellMaps Pipelines**

205 To evaluate the consistency of our modifications, we compared protein hierarchies generated by the
 206 baseline CellMaps pipeline and the Modified CellMaps pipeline across untreated and drug-treated
 207 conditions (Fig. 2). The baseline approach derives hierarchies from global image embeddings,
 208 whereas the Modified pipeline incorporates object detection and ViT-based single-cell embeddings.

209 For the untreated condition (Fig. 2a), the overlap between the two approaches was high: 95 proteins
 210 were shared (97.9% concordance), with only one protein (RACK1) unique to the baseline hierarchy
 211 and one (TUBB8) to the Modified hierarchy.

212 For Paclitaxel (Fig. 2b), 92 proteins were shared (96.9% overlap). Four proteins (CBX3, RPS3,
 213 SMARCA5, ZBTB7B) appeared only in the baseline pipeline, while one (SMARCA4) was unique
 214 to the Modified version. This indicates that the Modified pipeline preserves Paclitaxel-associated
 215 modules but slightly reshapes centrality and regulatory protein membership.

216 For Vorinostat (Fig. 2c), 93 proteins overlapped (95.9% concordance). Four proteins (CPT1A,
 217 DNMT1, DNMT3A, SRP14) were unique to the baseline pipeline, and none to the Modified ver-
 218 sion, suggesting that the Modified approach retains nearly all Vorinostat-associated proteins while
 219 simplifying the hierarchy.

220 In addition, we also performed comparison of the original pipeline and modified pipeline of two
 221 settings (Paclitaxel and Vorinostat). DenseNet/whole-image approach summarizes entire fields of
 222 view, which dilutes cell-level signal and tends to produce more centralized network modules and

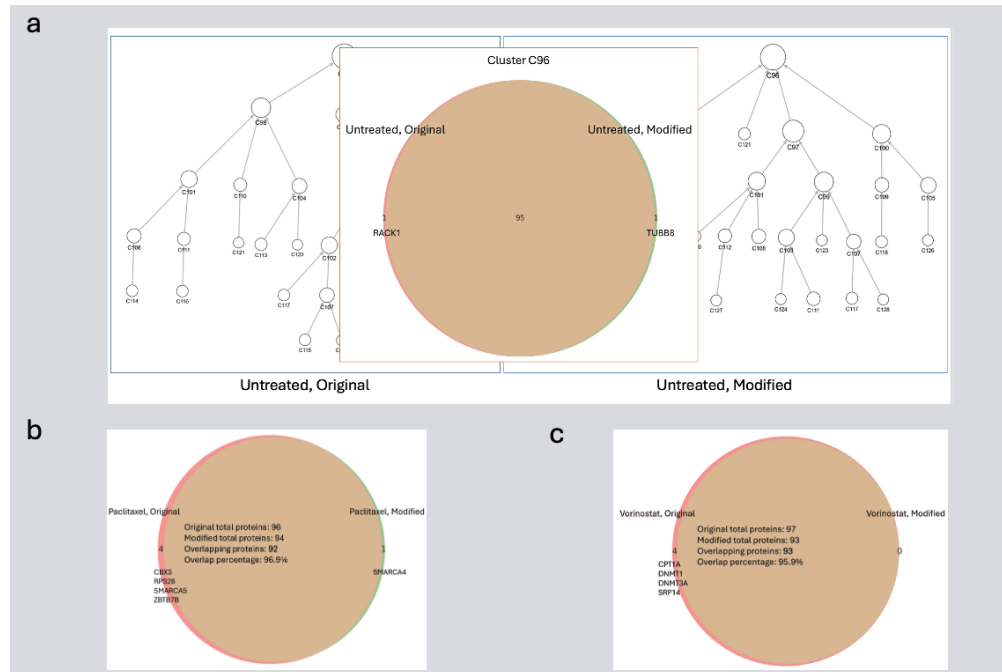


Figure 2: Comparison of baseline (Original) and Modified CellMaps hierarchies across conditions. (a) Untreated: 95 shared proteins (97.9% overlap), 1 unique to each pipeline. (b) Paclitaxel: 92 shared proteins (96.9% overlap), 4 unique to baseline, 1 unique to Modified. (c) Vorinostat: 93 shared proteins (95.9% overlap), 4 unique to baseline, none unique to Modified.

223 broader GO categories. The modified ViT/object-centric pipeline embeds individual cells, raising
 224 signal-to-noise, preserving heterogeneity, and yielding distributed hierarchies with more selective
 225 enrichment—i.e., it refines rather than replaces the original organization.

226 3.4 Drug-specific molecular reprogramming captured by the modified pipeline

227 We compared the modified networks for Paclitaxel and Vorinostat to resolve treatment-specific
 228 effects (Fig. 3). Both conditions preserved core chromatin and metabolic signatures, including
 229 strong enrichment in ATP-dependent chromatin remodeling (adenosine triphosphate-dependent), fatty
 230 acid metabolism, and nuclear components, confirming the stability of the modified pipeline across
 231 perturbations.

232 Distinct profiles emerged with each drug. Paclitaxel uniquely amplified pathways linked to long-term
 233 potentiation and oocyte meiosis, consistent with drug-induced disruption of signaling and cell cycle
 234 regulation. Vorinostat, in contrast, showed selective enrichment in the spliceosome and amino acid
 235 biosynthesis, aligning with its mechanism as a histone deacetylase inhibitor that broadly impacts
 236 transcriptional and RNA processing. These results highlight the pipeline’s capacity to preserve shared
 237 biological modules while sensitively resolving drug-specific molecular reprogramming.

238 4 Discussion

239 We present a cell-centric framework that links single-cell morphological embeddings to PPI features,
 240 capturing heterogeneity while preserving baseline structure. High concordance (97.9% overlap) and
 241 more selective GO enrichment show that object-level embeddings reduce noise and sharpen signal
 242 without loss of fidelity.

243 Methodologically, our contribution is not only a change in representation but also a transparent,
 244 agent-supported workflow: segmentation is executed via an interactive agent bridged to HPC, and
 245 embedding/integration/hierarchy steps proceed through audited, human-in-the-loop code generation

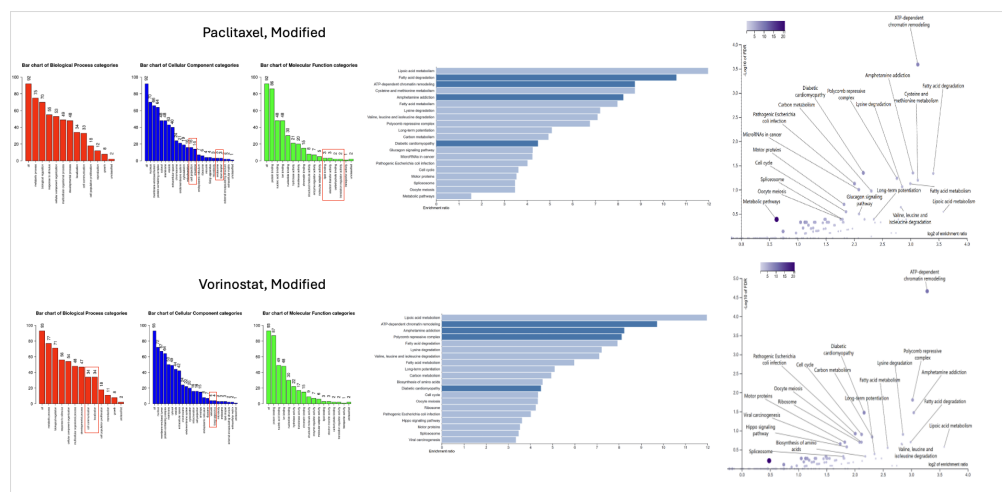


Figure 3: Functional enrichment profiles of Paclitaxel- and Vorinostat-modified networks. Bar plots (left) summarize Gene Ontology categories across biological process, cellular component, and molecular function. Enrichment ratios (center) and pathway significance plots (right) highlight shared chromatin and metabolic signatures while resolving drug-specific differences. Paclitaxel uniquely enriched long-term potentiation and oocyte meiosis, whereas Vorinostat emphasized the spliceosome and amino acid biosynthesis.

246 and execution. This orchestration emphasizes provenance, failure handling, and reproducibility,
 247 offering a practical template for agentic scientific computing in multimodal biology.

248 Relative to image-profiling pipelines that rely on whole-image aggregation or handcrafted features,
 249 the object-level strategy improves signal-to-noise and reduces spurious enrichments while main-
 250 taining global coherence. Unlike general cross-modal alignment methods, our framework targets
 251 morphology–PPI integration and operationalizes ontology-grounded evaluation within a unified
 252 workflow.

253 Our approach has several limitations. Segmentation metrics were not reported due to lack of ground
 254 truth in CM4AI, so evaluation relied on visual inspection. We also rely on ViT backbones not
 255 pretrained on fluorescence microscopy, which may miss domain-specific cues; domain-adapted
 256 pretraining could improve sensitivity. Enrichment analyses remain correlative and require orthogonal
 257 validation. Finally, while the agentic workflow improves traceability, it introduces operational risks
 258 that still need human oversight (e.g., User Interface actions, dependency drift).

259 Our framework may positively impact precision medicine by enabling reproducible, interpretable
 260 integration of single-cell imaging with protein networks, improving biomarker discovery and drug
 261 mechanism studies. Potential risks include bias in PPI resources, over-interpretation of correlative
 262 enrichments, dual-use concerns, and environmental costs of computation. These can be mitigated by
 263 open reproducible practices, human oversight of LLM-assisted steps, orthogonal biological validation,
 264 responsible licensing, and reporting compute usage.

265 5 Conclusion

266 In this study, we developed and applied the Modified CellMaps pipeline that integrates object-level
 267 microscopy embeddings with PPI embeddings to generate biologically interpretable hierarchical
 268 maps. By combining segmentation, ViT feature extraction, and molecular network embeddings, the
 269 workflow preserved the biological consistency of the original CellMaps approach while improving
 270 resolution and specificity.

271 Looking ahead, further improvements can be achieved by adopting larger or domain-adapted ViT
 272 models, incorporating additional omics layers (e.g., transcriptomics and phosphoproteomics), and
 273 conducting orthogonal experimental validation.

274 **References**

- 275 [1] Luck, K. et al. A reference map of the human binary protein interactome. *Nature* 580, 402–408 (2020).
- 276 [2] Huttlin, E. et al. Dual proteome-scale networks reveal cell-specific remodeling of the human interactome.
277 *Cell* 184, 3022–3040 (2021).
- 278 [3] Bray, M.-A. et al. Cell painting, a high-content image-based assay for morphological profiling. *Nat. Protoc.*
279 11, 1757–1774 (2016).
- 280 [4] Caicedo, J. et al. Data-analysis strategies for image-based cell profiling. *Nat. Methods* 14, 849–863 (2017).
- 281 [5] Chandrasekaran, S. et al. Three million images and morphological profiles of cells. *Nat. Methods* 21, 50–59
282 (2024).
- 283 [6] Szklarczyk, D. et al. The string database in 2023: protein–protein association networks and functional
284 enrichment analyses for any sequenced genome of interest. *Nucleic Acids Res.* 51, D638–D652 (2023).
- 285 [7] Qin, Y. et al. A multi-scale map of cell structure fusing protein images and interactions. *Nature* 600, 536–542
286 (2021).
- 287 [8] Cho, N. et al. Opencell: proteome-scale endogenous tagging enables the cartography of human cellular
288 organization. *Nat. Methods* 19, 845–856 (2022).
- 289 [9] Chen, S. et al. Maxfuse enables data integration across weakly linked single-cell modalities. *Nat. Biotechnol.*
290 42, 1843–1853 (2024).
- 291 [10] Nguyen, C. et al. Molecule–morphology contrastive pretraining (mocop) for drug discovery. *bioRxiv*
292 doi:10.1101/2023.05.07.539639 (2023).
- 293 [11] Dosovitskiy, A. et al. An image is worth 16x16 words: Transformers for image recognition at scale. In
294 *ICLR* (2021).
- 295 [12] Grover, A. et al. node2vec: Scalable feature learning for networks. In *KDD* (2016).
- 296 [13] Hamilton, et al. Inductive representation learning on large graphs. In *NeurIPS* (2017).
- 297 [14] Chen, T. et al. A simple framework for contrastive learning of visual representations. In *ICML* (2020).
- 298 [15] He, K. et al. Momentum contrast for unsupervised visual representation learning. In *CVPR* (2020).
- 299 [16] Sun, F.-Y. et al. Infograph: Unsupervised and semi-supervised graph-level representation learning via
300 mutual information maximization. In *ICLR* (2019).
- 301 [17] Radford, A. et al. Learning transferable visual models from natural language supervision. In *ICML* (2021).
- 302 [18] Chandrasekaran, S. N. et al. Jump cell painting dataset: morphological impact of thousands of chemical
303 and genetic perturbations. *bioRxiv* (2023).
- 304 [19] Gao, Y. et al. Maxfuse: Cross-modal integration via iterative co-embedding. *Nat. Methods* (2023).
- 305 [20] Sailem, H. et al. Mocop: Contrastive pretraining for morphology and molecular graphs. *bioRxiv* (2022).
- 306 [21] Lenkiewicz, J. et al. Cell mapping toolkit: an end-to-end pipeline for mapping subcellular organization.
307 *Bioinformatics* 41, (2025).

308 **Author contributions statement**

309 We used LLMs (ChatGPT 5, Gemini 2.5) as a co-pilot for planning, code drafting, and as an interactive
310 agent to launch segmentation. AI contributed to segmentation (LLM-guided detection and mask
311 generation), image feature extraction, and manuscript preparation (LaTeX structure and refinement).
312 All code was reviewed and executed by the authors on HPC, outputs were validated (e.g., overlap
313 statistics, GO/KEGG checks), biological interpretations were made by the authors, and the human
314 team assumes full responsibility for the results.

315 **Competing interests**

316 The authors declare that they have no conflicts of interest.

317 **Responsible AI Statement**

318 This work adheres to the NeurIPS Code of Ethics and the Responsible AI requirements of
319 Agents4Science. The AI system served as the primary contributor, generating code, drafting
320 manuscript sections, and executing experimental pipelines under human oversight.

321 We recognize potential risks, including (i) bias or incompleteness in public protein–protein interaction
322 resources, (ii) over-interpretation of agent-generated outputs without biological validation, (iii) dual-
323 use concerns in applying automated pipelines to sensitive biomedical data, and (iv) environmental
324 impact from compute requirements. Mitigation strategies include transparency of AI involvement,
325 open release of anonymized code and reproducible workflows, explicit human validation of outputs,
326 reporting of compute usage, and limiting analyses to publicly available, non-identifiable datasets.

327 The anticipated broader impacts include advancing reproducible multimodal biomedical AI, ac-
328 celerating discovery through interpretable agentic workflows, and lowering technical barriers for
329 interdisciplinary researchers while ensuring safe and responsible deployment.

330 **Reproducibility Statement**

331 We provide all materials required to reproduce our results.

332 **Code and Artifacts.** An anonymized repository with source code, experiment scripts, and run logs
333 is provided at [ANONYMIZED_REPO_URL].

334 **Data Access.** We use publicly available CM4AI resources (subset described in the paper: im-
335 munofluorescent microscopy for untreated, paclitaxel, and vorinostat conditions). The repo includes
336 a downloaded version of the dataset.

337 **Environment and Determinism.** Experiments were executed on an HPC cluster with NVIDIA
338 GPUs. We fix random seeds across numpy, torch, and Python (`seed=42`).

339 **Preprocessing and Pipelines.** The repository provides callable pipelines for (1) cell/object detection
340 and mask generation, (2) ViT-based single-cell feature extraction, (3) PPI embedding generation and
341 alignment, and (4) hierarchical analyses. Each stage has a corresponding Jupyter notebooks.

342 **Hyperparameters and Evaluation.** Default hyperparameters are reported in the paper.

343 **Compute Reporting.** For transparency, we log wall-clock time, GPU model/count in the paper.
344 This enables independent estimation of compute and energy cost.

345 **Licensing and Usage.** Code is released under a permissive license compatible with the dataset
346 terms (see LICENSE and dataset licenses referenced in the README).

347 **Additional information**

348 The source code is made public via the link [https://anonymous.4open.science/r/CM4AI-](https://anonymous.4open.science/r/CM4AI-56A4/README.md)
349 [56A4/README.md](https://anonymous.4open.science/r/CM4AI-56A4/README.md)

350 **A Technical Appendices and Supplementary Material**

351 Technical appendices with additional results, figures, graphs and proofs may be submitted with the
352 paper submission before the full submission deadline, or as a separate PDF in the ZIP file below
353 before the supplementary material deadline. There is no page limit for the technical appendices.

354 Agents4Science AI Involvement Checklist

355 1. **Hypothesis development:** Hypothesis development includes the process by which you
356 came to explore this research topic and research question. This can involve the background
357 research performed by either researchers or by AI. This can also involve whether the idea
358 was proposed by researchers or by AI.

359 Answer: B — AI-led ideation with human oversight/selection.

360 Explanation: ChatGPT proposed stepwise pipelines and brainstormed directions; humans
361 evaluated options, refined scope, and chose what to implement. AI organized ideas but did
362 not make autonomous decisions.

363 2. **Experimental design and implementation:** This category includes design of experiments
364 that are used to test the hypotheses, coding and implementation of computational methods,
365 and the execution of these experiments.

366 Answer: C — Mixed: AI-generated code & human-run execution.

367 Explanation: The LLM drafted segmentation and processing scripts and helped plan exper-
368 iments; one agent operated mostly automatically, while the other tasks were executed by
369 humans on the HPC, who handled failures, tuned parameters, and integrated outputs.

370 3. **Analysis of data and interpretation of results:** This category encompasses any process to
371 organize and process data for the experiments in the paper. It also includes interpretations of
372 the results of the study.

373 Answer: B — AI-led interpretation with human oversight.

374 Explanation: About 90% of the analysis and interpretation was performed with LLM support.
375 ChatGPT and Gemini organized, summarized, and contextualized the data outputs (e.g.,
376 pathway enrichments, cluster comparisons, visualizations), producing first-pass interpre-
377 tations. Humans reviewed, corrected possible hallucinations, and finalized the biological
378 narratives.

379 4. **Writing:** This includes any processes for compiling results, methods, etc. into the final
380 paper form. This can involve not only writing of the main text but also figure-making,
381 improving layout of the manuscript, and formulation of narrative.

382 Answer: B — AI-led drafting with human oversight/edits.

383 Explanation: The LLM produced drafts, LaTeX structure, and figure captions; humans
384 verified accuracy, corrected errors, and finalized the narrative.

385 5. **Observed AI Limitations:** What limitations have you found when using AI as a partner or
386 lead author?

387 Description:

388 **Observed AI Limitations: What limitations have you found when using AI as a partner**
389 **or lead author?**

390 • **Task execution.** Because our pipeline runs in Jupyter notebooks, many steps require
391 interaction with a web interface. The ChatGPT-provided agent performs well when
392 instructions are precise and can attempt to correct errors, though some issues may
393 persist and still require human intervention.

394 • **Idea generation.** ChatGPT is a strong brainstorming assistant; some ideas are genu-
395 inely valuable, but novelty and feasibility still require human vetting.

396 • **Manuscript writing.** Agents can deliver rigorous “harsh reviews” (via LLM API
397 calls) and, when combined, enable fast revision cycles. However, factual accuracy and
398 citation integrity must be checked by humans.

399 • **Interpretation of results.** AI can produce high-quality summaries and explana-
400 tions—especially for non-experts—but domain-specific nuances and causal claims
401 should be validated by human experts.

402 **Overall.** Multi-agent LLM workflows are promising and can accelerate research, but they
403 require careful oversight, verification, and error handling to be reliable at scale.

404 **Agents4Science Paper Checklist**

405 **1. Claims**

406 Question: Do the main claims made in the abstract and introduction accurately reflect the
407 paper's contributions and scope?

408 Answer: **[Yes]**

409 Justification: The Abstract/Introduction state the object-centric pipeline, agent-assisted
410 workflow, >95% hierarchy concordance, and drug-consistent GO findings, matching the
411 contributions shown later in Results.

412 Guidelines:

- 413 • The answer NA means that the abstract and introduction do not include the claims
414 made in the paper.
- 415 • The abstract and/or introduction should clearly state the claims made, including the
416 contributions made in the paper and important assumptions and limitations. A No or
417 NA answer to this question will not be perceived well by the reviewers.
- 418 • The claims made should match theoretical and experimental results, and reflect how
419 much the results can be expected to generalize to other settings.
- 420 • It is fine to include aspirational goals as motivation as long as it is clear that these goals
421 are not attained by the paper.

422 **2. Limitations**

423 Question: Does the paper discuss the limitations of the work performed by the authors?

424 Answer: **[Yes]**

425 Justification: Discussion notes ViT not pretrained for fluorescence, enrichment analyses are
426 correlative, and agentic workflow requires human oversight due to operational risks.

427 Guidelines:

- 428 • The answer NA means that the paper has no limitation while the answer No means that
429 the paper has limitations, but those are not discussed in the paper.
- 430 • The authors are encouraged to create a separate "Limitations" section in their paper.
- 431 • The paper should point out any strong assumptions and how robust the results are to
432 violations of these assumptions (e.g., independence assumptions, noiseless settings,
433 model well-specification, asymptotic approximations only holding locally). The authors
434 should reflect on how these assumptions might be violated in practice and what the
435 implications would be.
- 436 • The authors should reflect on the scope of the claims made, e.g., if the approach was
437 only tested on a few datasets or with a few runs. In general, empirical results often
438 depend on implicit assumptions, which should be articulated.
- 439 • The authors should reflect on the factors that influence the performance of the approach.
440 For example, a facial recognition algorithm may perform poorly when image resolution
441 is low or images are taken in low lighting.
- 442 • The authors should discuss the computational efficiency of the proposed algorithms
443 and how they scale with dataset size.
- 444 • If applicable, the authors should discuss possible limitations of their approach to
445 address problems of privacy and fairness.
- 446 • While the authors might fear that complete honesty about limitations might be used by
447 reviewers as grounds for rejection, a worse outcome might be that reviewers discover
448 limitations that aren't acknowledged in the paper. Reviewers will be specifically
449 instructed to not penalize honesty concerning limitations.

450 **3. Theory assumptions and proofs**

451 Question: For each theoretical result, does the paper provide the full set of assumptions and
452 a complete (and correct) proof?

453 Answer: **[NA]**

454 Justification: The paper presents an applied computational pipeline without formal theorems
455 or proofs.

456
457
458
459
460
461
462
463
464
465
466
467
468
469
470
471
472
473
474
475
476
477
478
479
480
481
482
483
484
485
486
487
488
489
490
491
492
493
494
495
496
497
498
499
500
501
502
503
504
505

Guidelines:

- The answer NA means that the paper does not include theoretical results.
- All the theorems, formulas, and proofs in the paper should be numbered and cross-referenced.
- All assumptions should be clearly stated or referenced in the statement of any theorems.
- The proofs can either appear in the main paper or the supplemental material, but if they appear in the supplemental material, the authors are encouraged to provide a short proof sketch to provide intuition.

4. Experimental result reproducibility

Question: Does the paper fully disclose all the information needed to reproduce the main experimental results of the paper to the extent that it affects the main claims and/or conclusions of the paper (regardless of whether the code and data are provided or not)?

Answer: [\[Yes\]](#)

Justification: Methods describe each stage with auditable prompts/seeds/checkpoints, and the paper links to anonymized code; dataset source and subset are specified.

Guidelines:

- The answer NA means that the paper does not include experiments.
- If the paper includes experiments, a No answer to this question will not be perceived well by the reviewers: Making the paper reproducible is important.
- If the contribution is a dataset and/or model, the authors should describe the steps taken to make their results reproducible or verifiable.
- We recognize that reproducibility may be tricky in some cases, in which case authors are welcome to describe the particular way they provide for reproducibility. In the case of closed-source models, it may be that access to the model is limited in some way (e.g., to registered users), but it should be possible for other researchers to have some path to reproducing or verifying the results.

5. Open access to data and code

Question: Does the paper provide open access to the data and code, with sufficient instructions to faithfully reproduce the main experimental results, as described in supplemental material?

Answer: [\[Yes\]](#)

Justification: CM4AI is publicly available and the manuscript provides an anonymous repository link for code.

Guidelines:

- The answer NA means that paper does not include experiments requiring code.
- Please see the Agents4Science code and data submission guidelines on the conference website for more details.
- While we encourage the release of code and data, we understand that this might not be possible, so “No” is an acceptable answer. Papers cannot be rejected simply for not including code, unless this is central to the contribution (e.g., for a new open-source benchmark).
- The instructions should contain the exact command and environment needed to run to reproduce the results.
- At submission time, to preserve anonymity, the authors should release anonymized versions (if applicable).

6. Experimental setting/details

Question: Does the paper specify all the training and test details (e.g., data splits, hyperparameters, how they were chosen, type of optimizer, etc.) necessary to understand the results?

Answer: [\[Yes\]](#)

506 Justification: Table 2 lists hyperparameters (ViT backbone, Node2Vec, feature dimension,
507 seeds, etc.), compute environment, and segmentation parameters, though optimizer and
508 training details are limited.

509 Guidelines:

- 510 • The answer NA means that the paper does not include experiments.
- 511 • The experimental setting should be presented in the core of the paper to a level of detail
512 that is necessary to appreciate the results and make sense of them.
- 513 • The full details can be provided either with the code, in appendix, or as supplemental
514 material.

515 7. Experiment statistical significance

516 Question: Does the paper report error bars suitably and correctly defined or other appropriate
517 information about the statistical significance of the experiments?

518 Answer: [No]

519 Justification: Results report overlaps and enrichment but do not provide error bars, confi-
520 dence intervals, or significance testing for the main comparisons.

521 Guidelines:

- 522 • The answer NA means that the paper does not include experiments.
- 523 • The authors should answer "Yes" if the results are accompanied by error bars, confi-
524 dence intervals, or statistical significance tests, at least for the experiments that support
525 the main claims of the paper.
- 526 • The factors of variability that the error bars are capturing should be clearly stated
527 (for example, train/test split, initialization, or overall run with given experimental
528 conditions).

529 8. Experiments compute resources

530 Question: For each experiment, does the paper provide sufficient information on the com-
531 puter resources (type of compute workers, memory, time of execution) needed to reproduce
532 the experiments?

533 Answer: [Yes]

534 Justification: The paper specifies use of Red Hat Enterprise Linux 7, two NVIDIA Tesla
535 P100 GPUs, 8 CPU cores (16 GB each), and approximate runtime (1 month).

536 Guidelines:

- 537 • The answer NA means that the paper does not include experiments.
- 538 • The paper should indicate the type of compute workers CPU or GPU, internal cluster,
539 or cloud provider, including relevant memory and storage.
- 540 • The paper should provide the amount of compute required for each of the individual
541 experimental runs as well as estimate the total compute.

542 9. Code of ethics

543 Question: Does the research conducted in the paper conform, in every respect, with the
544 Agents4Science Code of Ethics (see conference website)?

545 Answer: [Yes]

546 Justification: Work uses public data, documents human oversight (no autonomous LLM
547 decisions), and asserts author responsibility; no human subjects/patient data are involved.

548 Guidelines:

- 549 • The answer NA means that the authors have not reviewed the Agents4Science Code of
550 Ethics.
- 551 • If the authors answer No, they should explain the special circumstances that require a
552 deviation from the Code of Ethics.

553 10. Broader impacts

554 Question: Does the paper discuss both potential positive societal impacts and negative
555 societal impacts of the work performed?

556
557
558
559
560
561
562
563
564
565
566
567
568

Answer: [Yes]

Justification: Discussion now includes a Broader Impacts paragraph covering positive uses (precision medicine, reproducibility) and risks (bias, over-interpretation, dual-use, compute costs) with mitigation strategies.

Guidelines:

- The answer NA means that there is no societal impact of the work performed.
- If the authors answer NA or No, they should explain why their work has no societal impact or why the paper does not address societal impact.
- Examples of negative societal impacts include potential malicious or unintended uses (e.g., disinformation, generating fake profiles, surveillance), fairness considerations, privacy considerations, and security considerations.
- If there are negative societal impacts, the authors could also discuss possible mitigation strategies.